



This is a repository copy of *Investigating the effect of different adhesion materials on electrical resistance using a high pressure torsion rig.*

White Rose Research Online URL for this paper:

<https://eprints.whiterose.ac.uk/203322/>

Version: Published Version

Article:

Skipper, W. orcid.org/0000-0001-8315-2656, Nadimi, S., Gutsulyak, D.V. et al. (3 more authors) (2023) Investigating the effect of different adhesion materials on electrical resistance using a high pressure torsion rig. *Wear*, 532-533. 205116. ISSN 0043-1648

<https://doi.org/10.1016/j.wear.2023.205116>

Reuse

This article is distributed under the terms of the Creative Commons Attribution (CC BY) licence. This licence allows you to distribute, remix, tweak, and build upon the work, even commercially, as long as you credit the authors for the original work. More information and the full terms of the licence here:

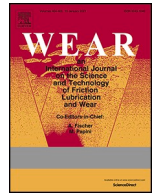
<https://creativecommons.org/licenses/>

Takedown

If you consider content in White Rose Research Online to be in breach of UK law, please notify us by emailing eprints@whiterose.ac.uk including the URL of the record and the reason for the withdrawal request.



eprints@whiterose.ac.uk
<https://eprints.whiterose.ac.uk/>



Investigating the effect of different adhesion materials on electrical resistance using a high pressure torsion rig

W. Skipper^{a,*}, S. Nadimi^b, D.V. Gutsulyak^c, J.G. Butterfield^d, T. Ball^e, R. Lewis^a

^a Leonardo Centre for Tribology, The University of Sheffield, Sheffield, S1 3JD, United Kingdom

^b School of Engineering, Newcastle University, Newcastle Upon Tyne, NE1 7RU, United Kingdom

^c L.B. Foster Rail Technologies Corp., 4041 Remi Place, Burnaby, BC, V5A 4J8, Canada

^d L.B. Foster Rail Technologies, Stamford Street, Sheffield, S9 2TX, United Kingdom

^e LNT Solutions, Isabella Road, Garforth, LS25 2DY, United Kingdom

ARTICLE INFO

Keywords:

Wheel/rail isolation
Adhesion materials
Sanding
Particle characterisation
Tribological testing

ABSTRACT

This paper presents an assessment of newly-developed conductive adhesion materials (Products A-E) in comparison to standard rail sand used in Britain. Current rail sand is an insulating material which can affect track circuits; newly-developed conductive materials could reduce the risk of this and allow for more material to be applied to further mitigate against low adhesion. The particles were characterised to determine their densities, and size and shape distributions. Bulk behaviour was assessed through three characteristics: angle of repose, bulk shear strength, and particle breakage index. Materials were then assessed using a high pressure torsion approach to measure their effects on adhesion and electrical resistance in dry, wet, and leaf contaminated conditions. It was found that all products produced better or equivalent conductivity compared to the currently used GB rail sand and that Product D and Product E should be considered for future field testing.

1. Introduction

The process of sanding has long been established as mitigation against low adhesion conditions in the wheel/rail contact. Low adhesion here is defined as conditions where the available traction in the wheel/rail contact is not sufficient for normal operation of the train; the minimum coefficient of traction needed to brake and accelerate being quantified as 0.09 & 0.2 respectively by Fulford [1].

Whilst the presence of these adhesion materials is necessary for reducing the impact of low adhesion, it can also lead to electrical isolation of train wheels from the track, particularly when rail head contamination is present, which can affect the functioning of track circuits. In the UK, track is split up into blocks, each of which forms a “track circuit” used for train detection. Within a section of track forming the circuit, which is typically bounded by insulated joints, a transmitter at one end sends an electrical signal to a detector at the other end. If a train is present, the track circuit is shorted out, thus the train is detected. When the wheel/rail interface is insulated by the presence of third body materials, there is a risk that the train can no longer be detected and problems arise [2], e.g. a near miss between a train and a car due to a level crossing functioning incorrectly [3]. A simple schematic of a track

circuit is presented in Fig. 1 for clarity.

Whilst there have been potential cases of track circuits failing due to the presence of sand [4] in the past there are also cases where the failure of the track circuit was due to contamination on the rail head [3]. It should be noted that in work conducted by The Rail Safety and Standards Board (RSSB) [5], using field data, the viability of applying sand during braking was assessed using RSSB’s Network Modelling Framework Safety Module. This approach calculated that reduction in risk of signals passed at danger (SPADs) was 170 times greater than the risk of isolation occurring, in fact, it was found that only 3% of isolations were caused by sanding with the rest coming from contamination. These findings suggest that whilst it is important to consider isolation when designing a sanding system, the ability of the system to remove contaminants is of much greater importance. However, these findings only apply to sand being applied at the current limit of 7.5 g/m [2] and if more sand was to be applied for further mitigation against low adhesion the risk of a loss of train detection may increase.

A full review paper focussing on the effect of particulate materials on restoring adhesion has been conducted by Skipper et al. [6]. In this review paper, it was observed that little work had been done to study the effect of particles on wheel/rail isolation and how particles could be

* Corresponding author.

E-mail address: W.Skipper@sheffield.ac.uk (W. Skipper).

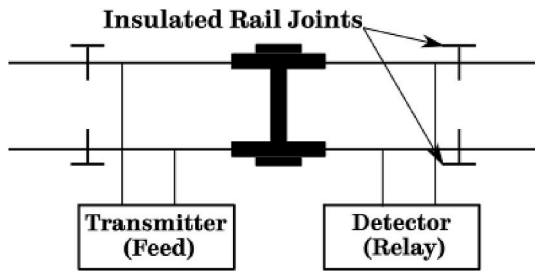


Fig. 1. Track circuit schematic.

Table 1
Summary of particle characterisation methodologies.

Characteristic	Technique	Ref
Particle Size	Sieve Analysis	[11]
Particle Shape	X-ray micro Computed Tomography	[12, 13]
Particle Density	Gas Jar	[11]
Angle of Repose	Plane Strain	[14, 15]
Bulk Shear Strength	Direct Shear Loading under varying Normal Stress	[16]
Particle Breakage	Measuring Evolution of Particle Size Distribution under 1D Compression	[17]

redesigned to overcome this. Two twin-disc studies [7,8] have been carried out, but these were quite limited in their scope as the contact conditions and size created an extreme case that would not be seen in the field and the recycling contact surface presented limitations.

The overall aim of this paper was to examine five newly-developed conductive sand consists (Products A-E) to assess their impact on adhesion and electrical resistance when compared with a standard grade of rail sand used in Great Britain (GB Rail Sand). To achieve this, the different materials were characterised to assess their key particle properties, in order to understand how the materials related to current standards and draw out possible relationships between characteristics and electrical conductivity in the contact. They were then applied to a high pressure torsion testing rig to measure their effect on adhesion and electrical resistance, the latter measurement was achieved by adapting the rig from previous work conducted by Evans et al. [9] & Skipper et al. [10].

2. Methodology

2.1. Particle characterisation

A range of techniques were utilised to assess particle characteristics. Single particle characteristics such as particle size and shape distribution and density were assessed. In addition, the bulk behaviours of particle types were assessed through three experiments: angle of repose, direct shear test, and one-dimensional compression. A summary of the techniques employed for measuring each characteristic has been included in

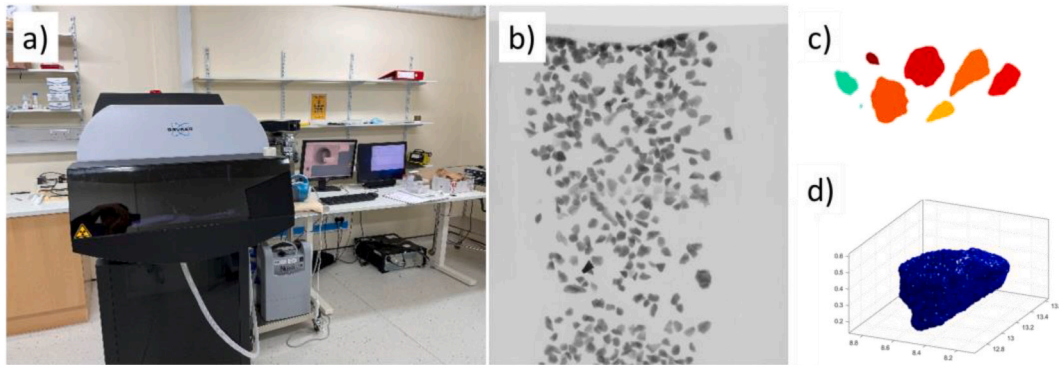


Fig. 2. (a) CT scanner used in this study, (b) raw radiograph of the GB rail sand, (c) labelled image, (d) 3D visualisation of the image.

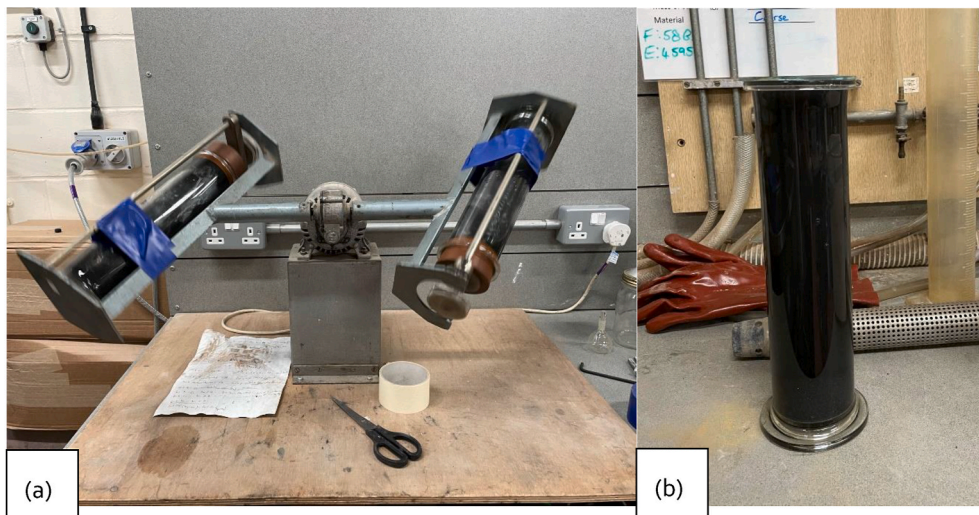


Fig. 3. Gas jar method to measure particle density, (a) sample tumbling, (b) gas jar used in this study.

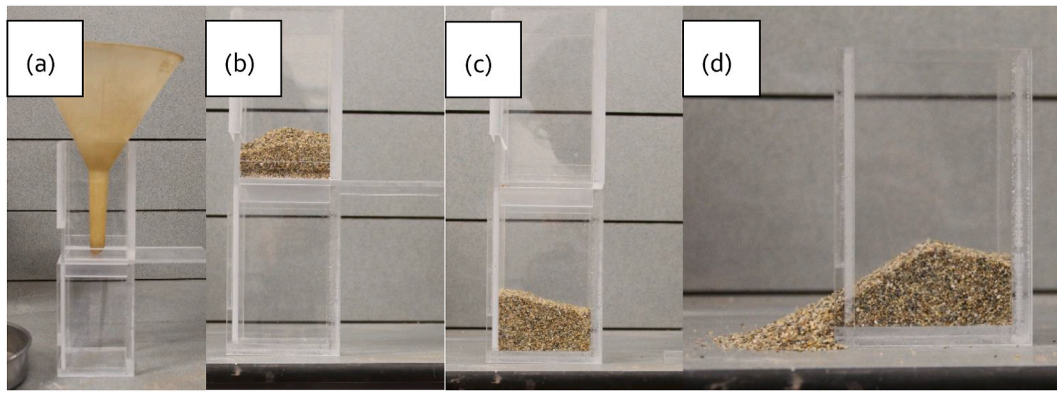


Fig. 4. Angle of Repose setup proposed by ISSMGE TC105. (a) The sample is air-pluviated using a funnel (b) The sample is fallen under gravity in the upper box and (c) Then fallen into the lower box under gravity to remove any fabric created during pluviation; (d) The side window is raised and a slope is formed.

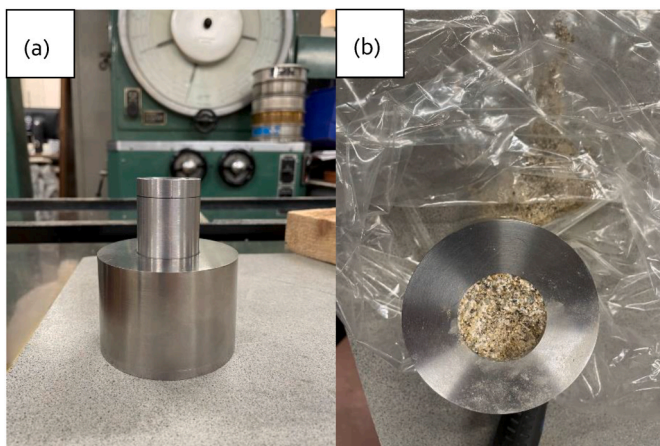


Fig. 5. (a) The cell designed for this experiment, (b) Crushed sand after the application of 600 MPa.

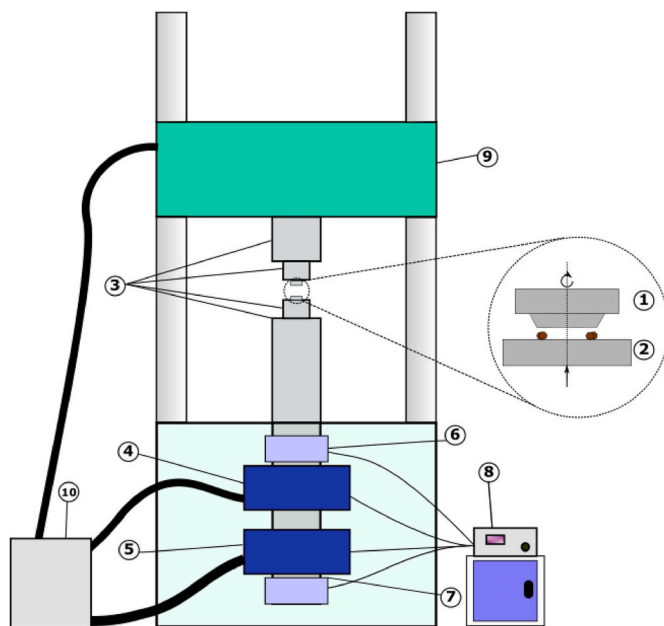


Fig. 6. Full schematic of the high pressure torsion rig [23].

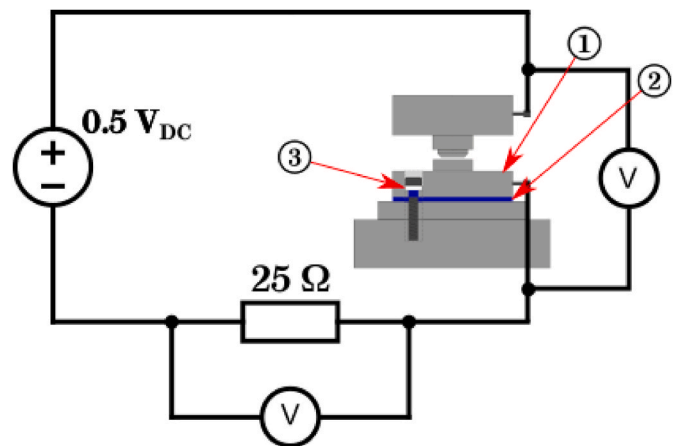


Fig. 7. Hpt set-up for conductivity measurements.

Table 1; in addition, respective references have been included for each technique which detail the methods for each.

2.1.1. Particle size

Particle size distribution of products was measured through sieve analysis following BS1377–2:1990 [18]. Material was riffled down to ~100 g samples to ensure a representative sample [19].

2.1.2. Particle shape

A set of X-ray micro-Computed Tomography (μ CT) scans were conducted to characterise particle shape parameters of the products in 3D. μ CT is a non-invasive, non-destructive method that allows the 3D visualisation of objects. The μ CT images obtained for this study were acquired using the SkyScan 1176 μ CT system, located in the Preclinical in Vivo Imaging Facility at Newcastle University Medical School, United Kingdom. The samples were scanned, with a source current of 45 kV and a voltage of 556 μ A. Image reconstruction generates greyscale cross-sectional slices with a voxel side length of 8.81 μ m (image resolution, where a voxel is to 3D imaging as a pixel is to 2D imaging). Each 3D image has 4000 \times 4000 \times 2480 voxels.

Blott and Pye [20] presented a review of all particle shape descriptors (including sphericity, elongation, flatness, and convexity) and the classification system (i.e. Zingg Plot) used in this work. Therefore, they are not elaborated on here.

Fig. 2 shows a view of the CT scanner used and the process of particle visualisation. The code SHAPE proposed by Angelidakis et al. [13] was used to characterise the shape of 3D avatars.



Fig. 8. Example of application amount for tests with a representative amount of material and with an over-application of material.

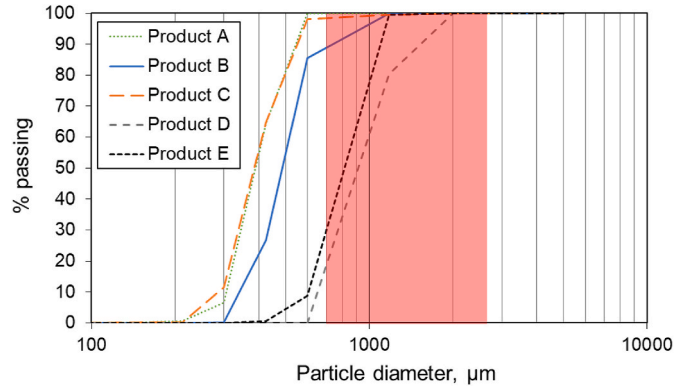


Fig. 9. Particle Size Distribution of five products used in this study obtained by sieve analysis. The red area shows the size range currently accepted by GMRT 2461 [2]. (For interpretation of the references to colour in this figure legend, the reader is referred to the Web version of this article.)

2.1.3. Particle density

The density of the particles was measured following BS1377–2:1990 gas jar method [18]. At least two specimens from each product (~200 g) were prepared by riffing, thereby ensuring a representative sample of particles for testing [19]. The specimens were oven dried at 105 °C for 24 h to remove moisture content and then tested at a room temperature of 21.2 °C. The specimens with known dry mass were tumbled in distilled water for 30 min (Fig. 3). Mass of water used to fill the gas jar with the material was measured against mass of water with no material. The averaged particle density of two tests was recorded, where the difference between two measurements was lower than 0.1 Mg/m³.

2.1.4. Angle of repose

The Angle of Repose (AoR) of a granular material is the slope relative to the horizontal plane to which a material can be piled. This is a quick and relative approach to measure flowability. The shallower the slope, the higher the flowability. There are several methods proposed in the literature to measure AoR [21]. In this study, a set-up proposed by the technical committee of the International Society for Soil Mechanics and Geotechnical Engineering (ISSMGE TC105) was adopted to test the AoR of the products as shown in Fig. 4 [14]. The camera used was a digital SLR camera Canon (Tokyo, Japan) EOS 60D 18 MP CMOS with EF-S 18-200-mm lens. A remote controller was used, and the shutter sound was muted to minimize any potential vibration. The open source software ImageJ was used to measure the angle [22]. Each test was repeated three times and averaged.

2.1.5. Bulk shear strength

In an AoR test, the material is falling and piling under gravity and may behave differently when subjected to external loading or in confined conditions. In particular, elongated and concave particles may show a higher degree of interlocking and may require higher shear

loading to flow. To quantify bulk shear behaviour under normal loading, the direct shear test was adopted following BS1377–7:1990 [16]. The test was performed by horizontally deforming a ~200 g sample in a 60 × 60 mm² box with a controlled strain rate of 1 mm/min while the specimen was subjected to vertical (normal) loading at 18, 40, 96, and 151 kPa.

2.1.6. Particle breakage

The products were subjected to 600 MPa one-dimensional compression to study their breakage index, which is a measure to quantify the number of fines/fragments produced after the compression of particles. Sand particles (~50 g) were poured into a cell with a 36 mm internal diameter and 22 mm thickness made of D2 steel. A piston was placed on the top of the sample and was compressed up to 600 MPa (610 kN) as shown in Fig. 5.

To quantify the breakage index, different measures have been recommended in the literature. Here, we report Marsal's [17] breakage index (B_m) which is:

$$B_m = \sum_{n=1}^i \Delta p d_n \quad \text{Equation 1}$$

where $\Delta p d_n$ is the positive difference in percentage by weight of material retained on the n th sieve, when the grading before and after a crushing test are compared.

2.2. High pressure torsion

A high pressure torsion (HPT) rig was used for assessing adhesion and electrical resistance under a range of contact conditions. A schematic of the HPT is shown in Fig. 6. The top and bottom specimens (1 & 2 respectively) were cut from R8T wheel and R260 rail respectively and were fixed into specimen holders (3). Initially, the specimens were out of contact, but were brought together during testing and a normal pressure of 600 MPa was applied using the axial hydraulic actuator (5). The specimen faces were then rotated against each other using a rotational hydraulic actuator (4). The third body layers being applied into the contact between the wheel and rail specimen change the amount of torque needed to turn through a set sweep length (0.4 mm), and the coefficient of traction is calculated from the ratio of the shear stress and the normal stress. A full description of the standard HPT methodology is available in work by Evans et al. [9] and traction results can be used to parameterise the extended creep force model and make predictions of full-scale behaviour [9].

A 600 MPa contact pressure was used to simulate light vehicles of ~80 kN axle load [24]. A light vehicle represents a worst-case scenario, where a lighter vehicle is less able to break down contaminants in the wheel/rail contact.

For this work, a 0.5 V_{DC} circuit was set up to measure conductivity between the wheel and rail specimens; a schematic of this has been included in Fig. 7. The value of 0.5 V_{DC} was chosen so as to represent the worst-performing track circuit found in UK rail operations, i.e. low voltage DC. 79% of wrong side track circuit failures in Great Britain

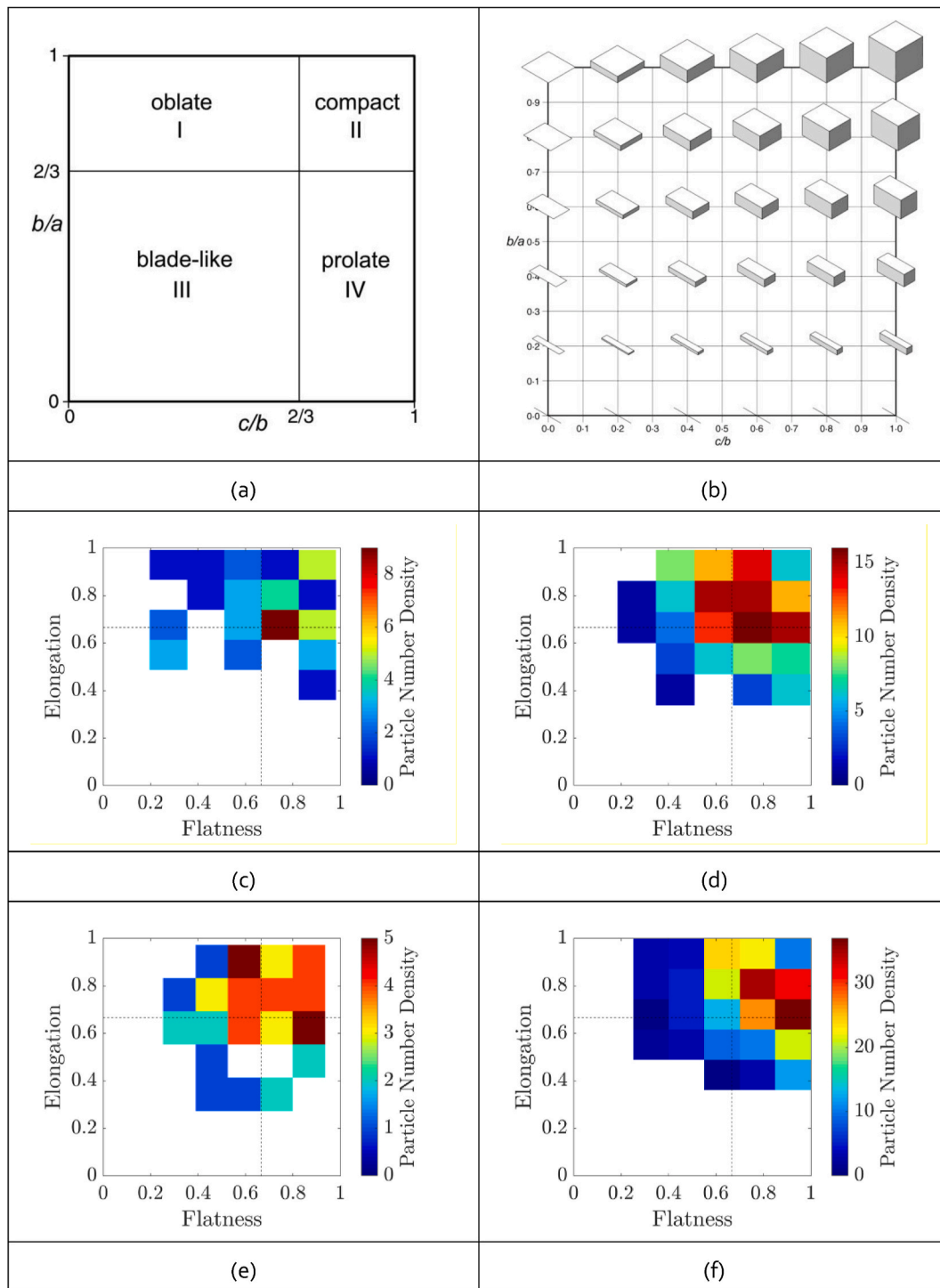


Fig. 10. (a) The shape classification system of Zingg [26]; (b) Graphical representation of Zingg Plot; (c) GB rail sand, (d) Product B, (e) Product D, and (f) Product E Shape Distribution on Zingg Plot.

between 2012 and 2022 occurred on DC circuits, despite making up just 63% of all track circuits [25].

A sub-schematic of the insulated rig has also been included in Fig. 7; the bottom sample holder (1) was isolated using a polythene layer (2) and the bolts were insulated with electrical tape and nylon washers (3).

Tests were conducted in dry, wet, and leaf contaminated conditions. These conditions were created in the same manner as [23], where 20 μ l of distilled water was applied to create wet conditions and Sycamore leaf powder and 40 μ l of distilled water were used to create leaf contaminated conditions.

Each adhesion material was tested at representative amounts of 7.5 g/m [2] (~25 mg of material per test) and with an amount of material needed to physically separate the top and bottom HPT specimens (i.e. enough material so that the contact is flooded with adhesion material). An example of the application amounts used has been included in Fig. 8. Two tests were conducted for each contact condition, with three passes over each application of material for each test.

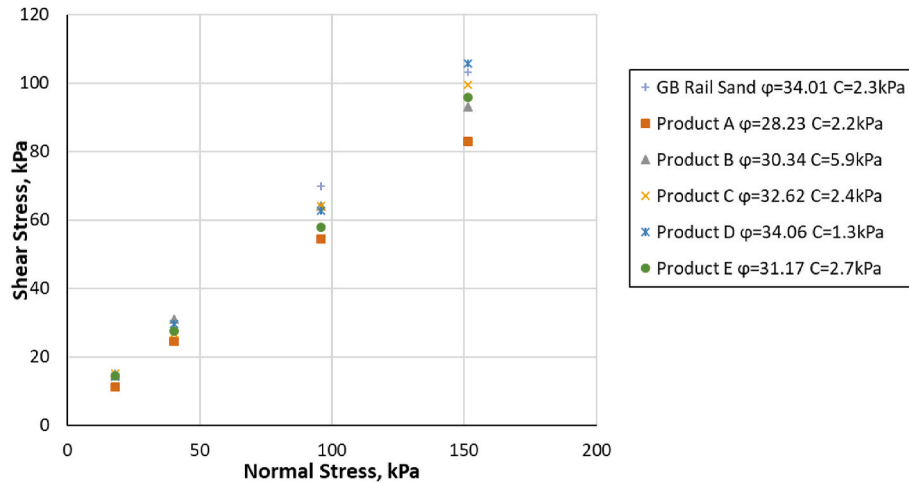


Fig. 11. Shear stress versus normal stress obtained from direct shear tests on six samples under 18, 40, 96, and 151 kPa normal loading. The values of bulk friction angle and cohesion are reported in the figure legend.

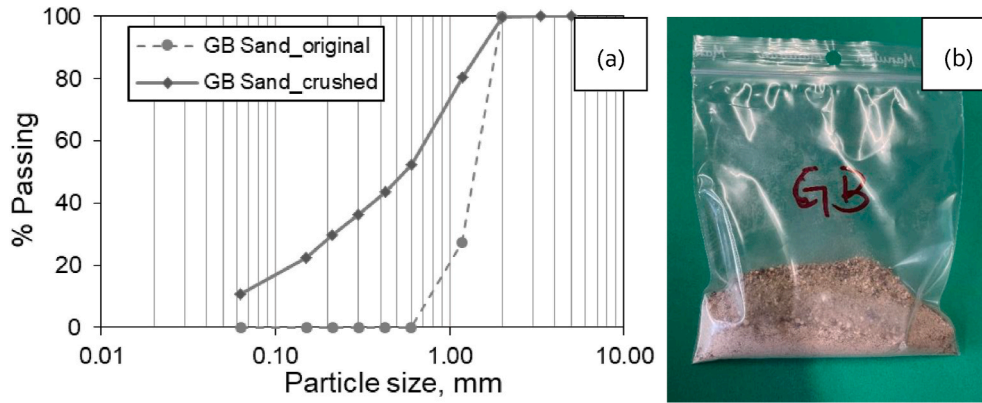


Fig. 12. Example of: (a) PSD curve of GB rail sand before and after compression, (b) Fine powders produced after compression.

Table 2
Summary of particle characterisation measurements.

Material		GB	A	B	C	D	E
Size D50 (μm)		1437	380	490	380	900	810
Particle Shape	Compact	36%	–	37%	–	35%	53%
	Flat	32%	–	30%	–	35%	21%
	Elongated	26%	–	25%	–	19%	23%
	Bladed	6%	–	8%	–	11%	3%
Density (Mg/m ³)		2.61	3.84	3.81	3.07	3.75	4.46
AoR (°)		28.6	31.9	32.3	31.2	29.9	34.1
Bulk Shear Strength	Friction Angle	34.01	28.23	30.34	32.62	34.06	31.17
	Cohesion (kPa)	2.3	2.2	5.9	2.4	1.3	2.7
Particle Breakage Index		0.954	–	–	–	1.121	1.164

3. Results

3.1. Particle characterisation

The results of sieve analysis for the newly developed products are included in Fig. 9, where the highlighted region represents the size range of rail sand currently used in Great Britain [2]. This size range was set due to many factors, one such issue being compatibility with current sanding systems. As can be seen, products D and E are partially in the proposed range and the rest of the products are finer than the currently accepted range (though this does not necessarily guarantee they'll be incompatible with current sanding systems).

Zingg plots have been included in Fig. 10, to demonstrate the

relationship between measured particles' dimensions (named "a", "b", and "c" in Fig. 10a and b). It can be seen that the naturally formed sand is less distributed in comparison with products under investigation. This can be attributed to the fact that natural materials have been eroded and rounded during their geological history. The majority of particles are in the "compact" region of the Zingg chart and show very similar shape distribution.

The shear stress required to flow under different normal stresses is plotted in Fig. 11. The slope of the linear trend line is called bulk friction angle (φ) and the intercept with y-axis is called cohesion (c). Product D shows a very similar bulk friction value to GB rail sand, whilst products A, C, and E show similar values of cohesion to GB rail sand.

A typical example of the particle size distributions before and after

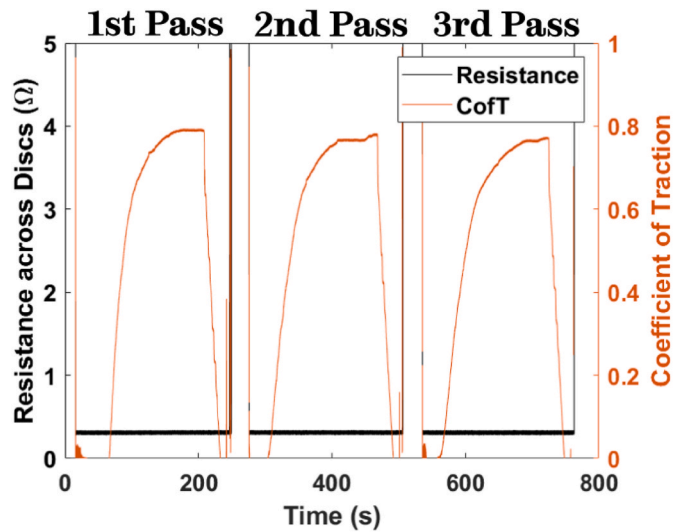


Fig. 13. Example of HPT Data from Dry Test with no Application of Adhesion Material.

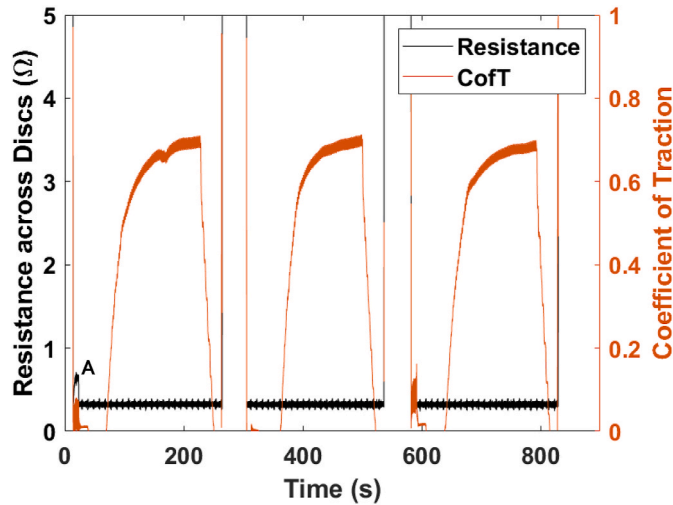


Fig. 14. Example of Test Data from Tests conducted in Dry Conditions with Adhesion Material Applied (GB Rail Sand in this Instance).

being subjected to the breakage index test is included for GB rail sand in Fig. 12. All tested materials exhibited a large drop in particle size after crushing.

A summary of all the particle characterisation measurements recorded as part of this project is included in Table 2. Significant differences in particle size and density between the materials were apparent, especially in comparison with GB rail sand, which had the largest particle size and smallest density; little difference was observed between respective particle shapes. Differences in angle of repose (AoR) suggest the flowability of different materials varies, with GB rail sand proving the most flowable and Product E the least i.e. GB rail sand will be least likely to jam up in the sand hopper. Characterisation of bulk shear strength found GB rail sand and Product D were able to support the highest level of shear stress, whilst Product B was the most cohesive. Products D & E were found to be more susceptible to breakage in comparison to GB rail sand.

3.2. High pressure torsion

As an example of raw data acquired from an HPT test, Fig. 13 has

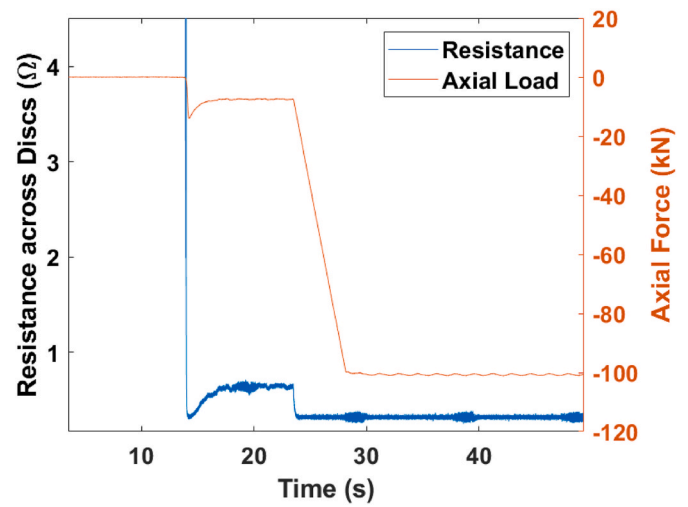


Fig. 15. Resistance in HPT Contact upon Initial Crushing of Particles (GB Rail Sand in this Instance).

been included; data from three passes of the wheel specimen over the rail specimen is included and demonstrates the appearance of a clean contact, with a high peak coefficient of traction (CofT) and very low electrical resistance throughout. Coefficient of traction is defined as the ratio between shear stress and normal pressure in the HPT contact. Between each pass, the specimens were separated and turned to a new position. For tests with adhesion material present, three test passes were performed for each application i.e. a 1st pass on freshly applied material, then the 2nd pass on the same, crushed, material, and the third pass on the same material again.

The measured coefficients of traction in Fig. 13 are noticeably high, especially compared to real-world measurements of rail adhesion, where values of 0.35–0.5 are typical. However, this is not unusual with regard to laboratory testing where traction values for steel-on-steel have been measured as greater than 0.45 [27–29], probably due to tighter control over contaminants and cleaning of specimens compared to the real world.

In addition, the HPT test is run at very low speeds, so there is little effect of temperature reducing traction further. Furthermore, it is possible to link HPT data to predictions of real-world behaviour by using an approach of parameterising the ECF model with HPT data [9].

3.2.1. Representative amounts

The following section includes the results of HPT tests conducted with a representative 7.5 g/m of adhesion material applied to the HPT contact.

In dry conditions, all materials produced no change in resistance behaviour as compared to a clean, dry contact (Fig. 13) for the majority of the test sweep, Fig. 14 shows an example test in dry conditions when adhesion material was applied.

There was an initial increase in resistance upon the particles first being crushed, Fig. 15 illustrates this effect and is marked with an “A”. As further axial load (normal force) was applied and the particles were further crushed, the resistance decreased to that of a clean contact.

Whilst resistance measurements were consistent, adhesion behaviour changed considerably from one material to the other in dry conditions. Fig. 16 presents the average peak coefficient of traction to some extent in dry conditions, but not to the extent that they created low adhesion (0.09 for braking, and 0.2 for acceleration according to Fulford [1]). GB rail sand and product E produced traction slightly below that of the unsanded contact. Products A-D all produced even lower adhesion, with Products A, B, and D all showing a reduction in traction with subsequent passes, this effect being most apparent for Product A. The values, however,

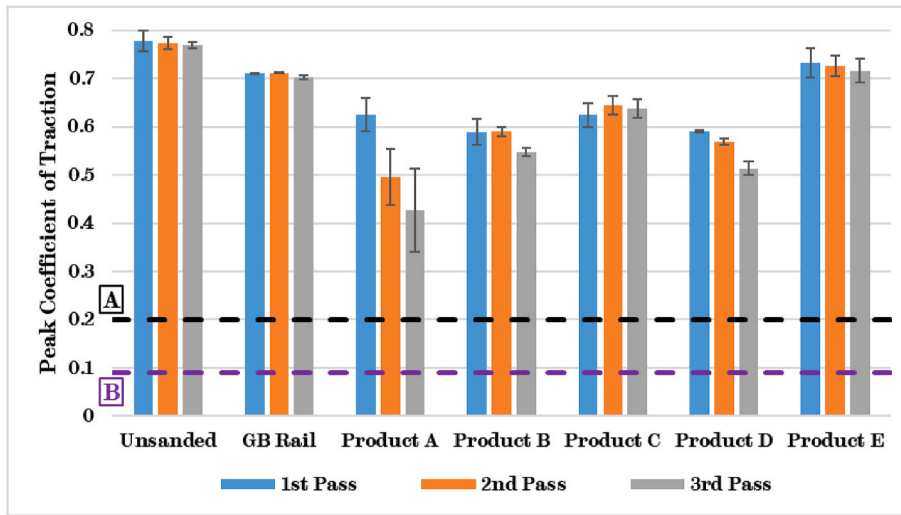


Fig. 16. Peak Coefficient of Traction in Dry Conditions for All Tested Adhesion Materials; (Line A) Minimum Level of Adhesion required for Acceleration, (Line B) Minimum Level of Adhesion required for Braking [1].

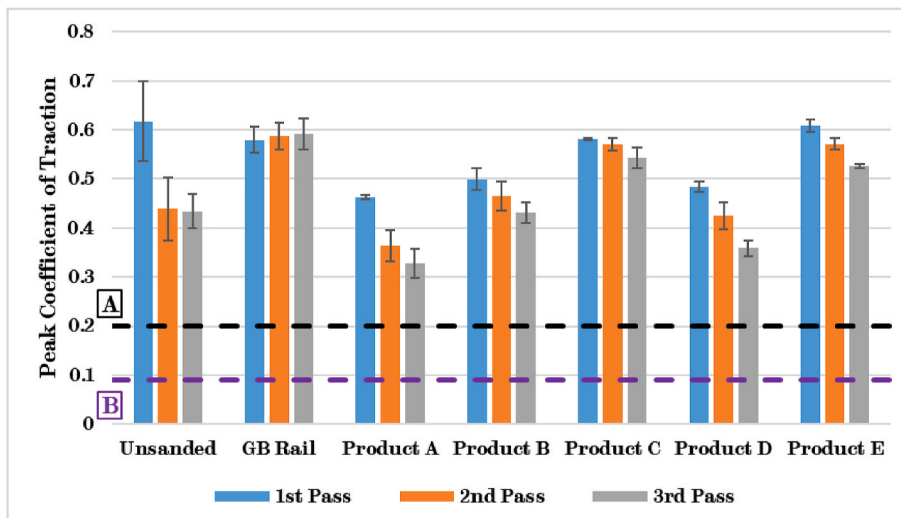


Fig. 17. Peak Coefficient of Traction in Wet Conditions for All Tested Adhesion Materials; (Line A) Minimum Level of Adhesion required for Acceleration, (Line B) Minimum Level of Adhesion required for Braking [1].

remained above the safe threshold for braking and acceleration. Product A also appeared to have the greatest degree of variation in measured traction, especially as the number of passes increases. This may be due to the manner in which Product A degrades over multiple applications of normal and shear load. The amount of variation suggests this may be a probabilistic phenomenon, however, as particle characterisation tests in section 3.1 were conducted on initially uncrushed material, they do not give sufficient evidence to infer behaviour of the degraded material.

In wet conditions, all materials produced no change in resistance behaviour as seen with a clean, dry contact (see Fig. 13). The different adhesion materials did affect the adhesion in the contact, as can be seen in Fig. 17. No material produced significant low adhesion in wet conditions, and some acted to increase traction compared to the wet, unsanded case. GB rail sand and product E produced the highest traction, with the former being the only material to not see any decrease in traction with the number of passes. Product C produced slightly lower traction than GB rail sand and did not see a large drop in traction between passes. Products A, B, and D produced similar peak traction values initially, though Product A reduced relatively sharply in comparison to B & D between the first and second pass.

Contrary to dry and wet conditions, the application of adhesion materials had a marked effect on resistance in the leaf contaminated contact. Unlike dry and wet conditions, the unsanded case generated much higher resistance in the contact (see Fig. 18).

Fig. 19 represents the relative amount of time each test condition spent at a given resistance value; in the unsanded case, resistance values were between 1000-10,000 Ω throughout the test runs.

All newly-developed products reduced resistance to some extent, some even reduced resistance to similar levels as seen in the clean contact. GB rail sand mostly produced high levels of resistance, though there was a spread in recorded resistance values over several levels of magnitude. Product E produced slightly lower resistance values, but overlapped with data for GB rail sand. Products C & D produced resistance values such that the majority of the time was spent at resistance values similar to that of a clean contact. Products A & B also reduced resistance to that of a clean contact, but the recorded resistance values were more varied throughout the test runs.

All adhesion materials increased adhesion in the contact by comparison to the unsanded, leaf contaminated case, though all materials also saw a slight reduction with number of passes. All materials

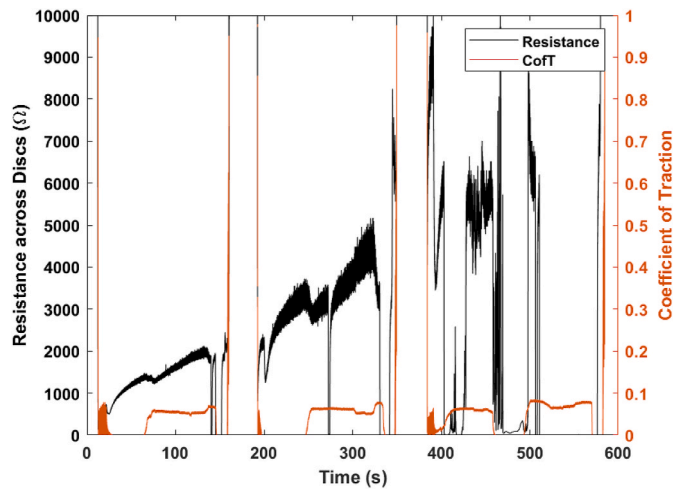


Fig. 18. Example of HPT Data from Leaf Contaminated Test with no Application of Adhesion Material.

produced adhesion values above the minimum adhesion level needed for braking, as can be seen in Fig. 20. It should also be noted that no material increased adhesion above 0.2 i.e. the minimum adhesion needed for acceleration.

The data acquired from this test method has indicated that there is scope for increasing the electrical conductivity of adhesion materials, whilst maintaining an adequate degree of mitigation against low adhesion conditions when applying material at the current maximum permitted amount in Great Britain (7.5 g/m).

3.2.2. Over-application

The following section includes the results of HPT tests conducted with an over-application (complete coverage of the bottom specimen) of adhesion material in the HPT contact.

In dry conditions, it is unsurprising that in the unsanded case, the resistance measured is the same as that of a clean contact throughout the test runs, as is illustrated in Fig. 21. When over-applied, all materials had some effect on resistance measurements, notably GB rail sand appears to have increased resistance measurements to very high levels. All other materials had less of an effect, with none creating resistance values > 10 Ω.

With the exception of product E, all over-applied materials reduced

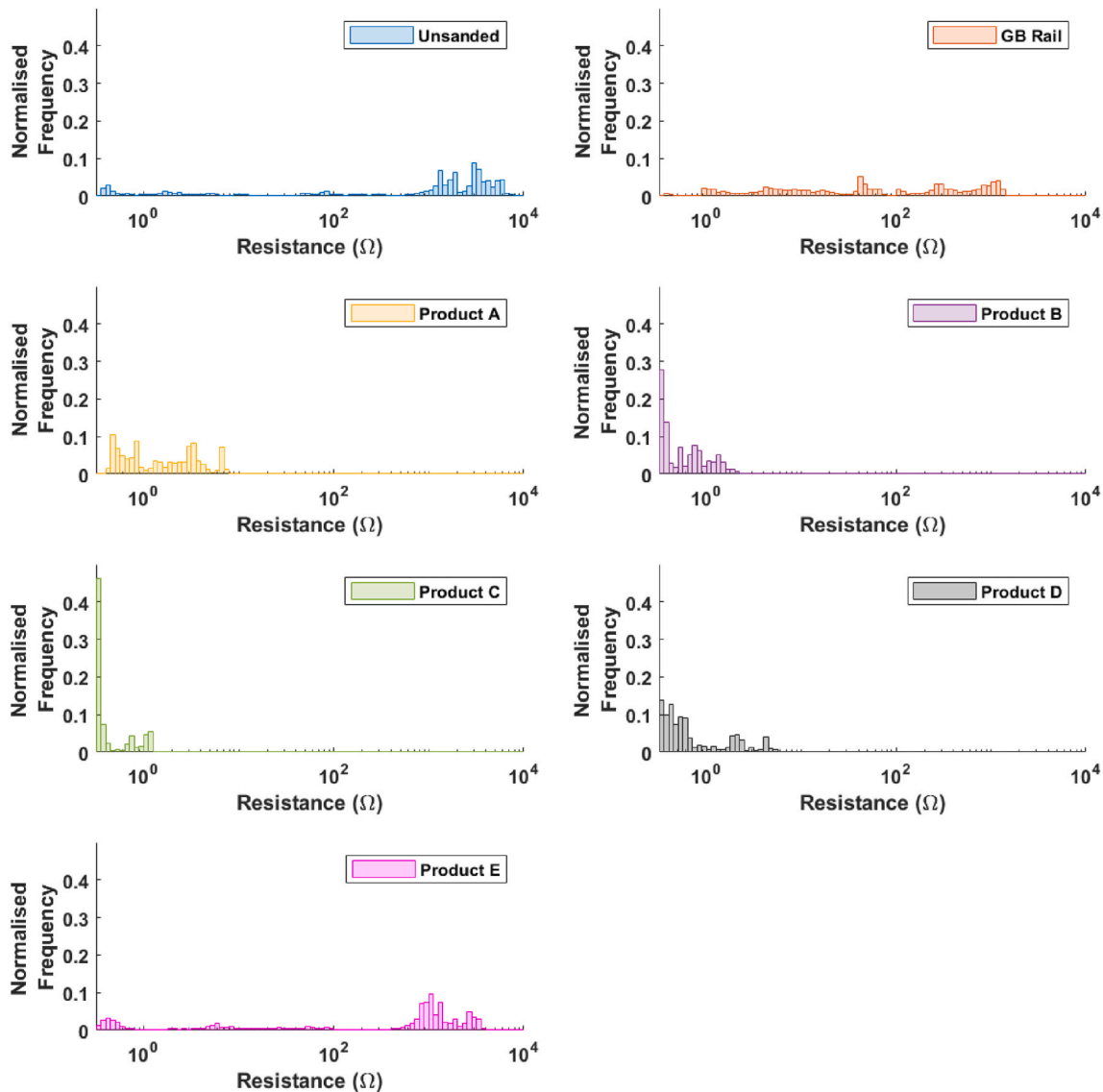


Fig. 19. Histogram plots of time the HPT contact spent at a given resistance in leaf contaminated conditions with representative adhesion material application.

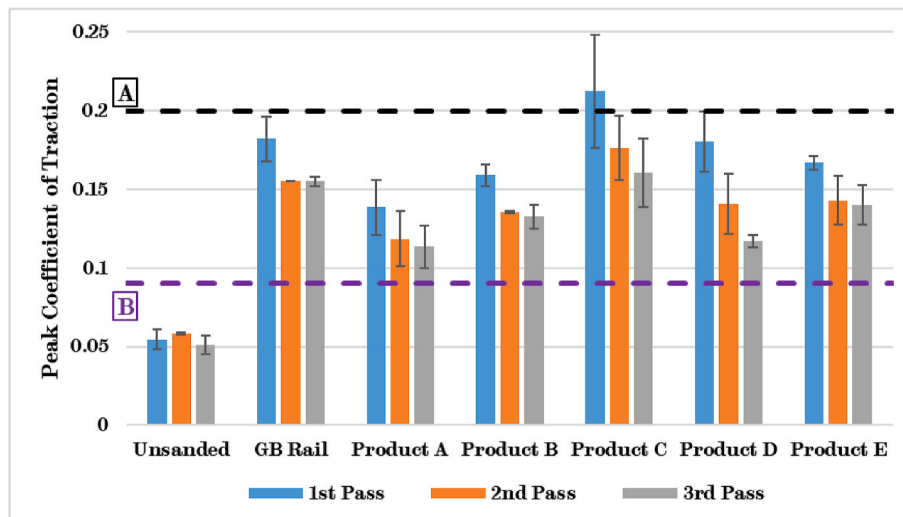


Fig. 20. Peak Coefficient of Traction in Leaf Contaminated Conditions for All Tested Adhesion Materials; (Line A) Minimum Level of Adhesion required for Acceleration, (Line B) Minimum Level of Adhesion required for Braking [1].

traction compared to unsanded conditions, though not to the extent that low adhesion conditions were created, see Fig. 22. As seen when representative amounts of material were applied, Product A saw a sizable drop in peak traction with increasing passes.

Compared to dry conditions, the spread of measured resistance values is much greater in wet conditions with an over-application of material, as can be observed in Fig. 23 (the unsanded case was at the level of a clean contact at all times and removed from the plot for clarity). GB rail sand and product E produced high resistance values for the entirety of their respective test runs. Other products mostly stayed $<10 \Omega$, with some materials partly reaching clean contact conditions, notably Product D spends a lot of time at these resistance values.

The overall peak traction trends are similar in wet conditions to what was observed in dry conditions though at lower adhesion values, with the exception of product E which was reduced somewhat. In Fig. 24 it can be seen that no material significantly improves peak traction when over-applied and Product A even created an adhesion value below 0.2 (the required adhesion level for acceleration).

Regarding leaf contaminated conditions, in Fig. 25 it can be seen that GB rail sand and product E made little difference to the measured resistance values compared to the unsanded case. Products A-D improve the resistance values observed to $<10 \Omega$, with product C producing some resistance values akin to a clean contact. Generally, the resistance is higher when adhesion material was over-applied than applied representatively (see Fig. 19).

All adhesion materials increased the peak coefficient of traction in the leaf contaminated HPT contact, as illustrated in Fig. 26. The overall trend between adhesion materials and peak traction is similar here, as for representative applications of material (see Fig. 20), though adhesion levels were generally higher.

It was observed that electrical resistance was higher in all conditions when adhesion material was over-applied in contrast to when it was applied at a representative, 7.5 g/m. All adhesion materials, applied representatively, did not alter resistance from that seen in a clean contact in both dry and wet conditions, though there were noticeable differences between materials in a leaf contaminated contact. Some of the newly-developed materials produced lower resistances in certain conditions than the GB rail sand and no newly-developed product produced higher resistance when compared to GB rail sand (which is currently approved for use on the railway in Great Britain).

In dry and wet conditions, adhesion was lowered when material was over-applied in comparison to when it was applied representatively, this was the opposite in leaf contaminated conditions. No adhesion material

created low adhesion in any test condition or application amount.

4. Discussion

Particle characterisation work identified key differences between new products and the GB rail sand currently in use. Whilst differences compared to GB rail sand do not necessarily mean a prospective new particle will not perform as well as GB rail sand in the wheel/rail contact, it does increase the chances of incompatibilities with current sanding standards and equipment. Bearing this in mind, products D & E appear most similar in terms of particle size and product D has a similar angle of repose. In addition, products C & D produce similar bulk shear strength to GB rail sand.

Whilst the HPT has been used in the past to assess traction, there was novelty in this work adapting the rig for measuring electrical conductivity. Previous twin-disc studies have noted the recycling layer of material and small contact size as limitations of the twin-disc method, limitations that the HPT did not possess. This work was successfully able to measure differences in electrical conductivity between different particle types and was especially effective at highlighting the possible risk of leaves and GB rail sand causing wheel/rail isolation.

The HPT tests showed that product A produced consistently lower peak coefficients of traction across all conditions, with a decrease in traction seen over multiple passes. Product C consistently produced marginally higher traction than the other particles, which all produced similar traction levels. Products B, C, and D all generally produced the lowest amount of resistance in the contact, producing resistance values approaching that of a clean contact in leaf contaminated conditions when applied at representative amounts.

The differences in performance during HPT testing are due to a combination of the particle characteristics and the composition of the materials. Previous work on the HPT [23] found relationships between traction in the contact and particles' size, shape, and hardness. It was observed that harder particles were correlated with higher traction in dry, wet, and leaf contaminated conditions, particle circularity was positively correlated with traction in dry and wet conditions, whereas the opposite held true in leaf contaminated conditions; and there existed an optimum particle size in leaf contaminated conditions. Products C & D are the same material (i.e. identical hardness), with product C being the smaller of the two (see Fig. 9), product C also produced higher traction values in the leaf contaminated contact, suggesting it was closer to the optimum particle size. In addition, products A-D were formed from coating a non-conductive, base material with a conductive

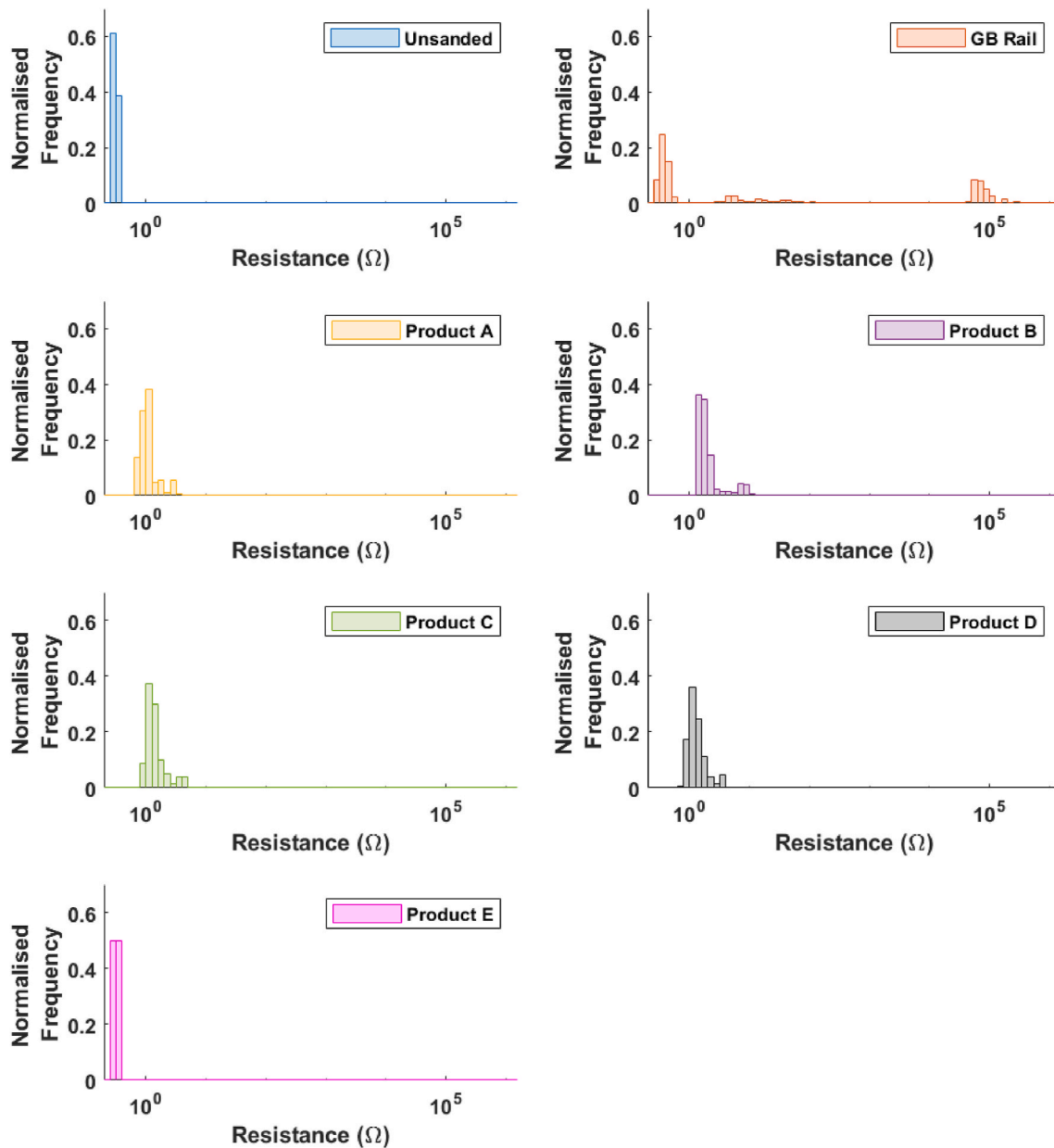


Fig. 21. Histogram plots of time the HPT contact spent at a given resistance in dry conditions with adhesion material over-application.

material; of these products A was made of the least hard base material and subsequently consistently produced lower traction in all conditions. In addition, product E consistently produced relatively high traction and was also made of a relatively hard constituent material. As all the particles were of a similar shape (see Fig. 10), this is not thought to have had an impact on differences in traction between the materials. Due to all newly developed products having a conductive constituent material, they were all able to produce lower or equal electrical resistance in the contact compared to GB rail sand.

Due to their respective performances in HPT testing and their characteristic similarity to GB rail sand, Products D & E have been identified as particles of interest for further field testing. This field testing will aim to validate findings from these laboratory experiments with a real track circuit and wheel/rail contact.

5. Conclusions

In this paper, GB rail sand and five newly-developed products

designed to aid conductivity in the wheel/rail interface were assessed for their particle characteristics, tribological performance, and effect on electrical conductivity. Part of this assessment utilised a new test method for assessing electrical conductivity in a high pressure tribological contact, i.e. the HPT method.

All the adhesion materials mitigated against low adhesion, both when applied at representative amounts and when over-applied, and in no circumstances was low adhesion produced when adhesion materials were present in the contact (below 0.09, though some instances of adhesion falling below 0.2 when products were applied in wet and leaf contaminated conditions did occur). No newly developed product produced higher electrical resistance in the contact than GB rail sand, and in some conditions, some of the newly-developed products produced much lower resistance. Some products even produced electrical resistances similar to that of a clean contact, even in leaf contaminated conditions.

Based on particle characterisation and respective performances during HPT testing, products D & E were deemed of interest for further testing, alongside GB rail sand to act as a control. This further testing

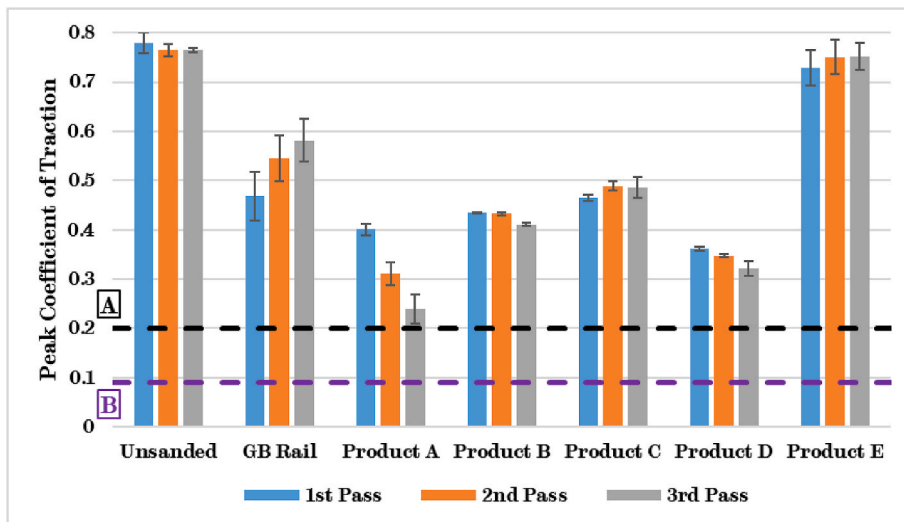


Fig. 22. Peak Coefficient of Traction in Dry Conditions for All Tested Over-Applied Adhesion Materials; (Line A) Minimum Level of Adhesion required for Acceleration, (Line B) Minimum Level of Adhesion required for Braking [1].

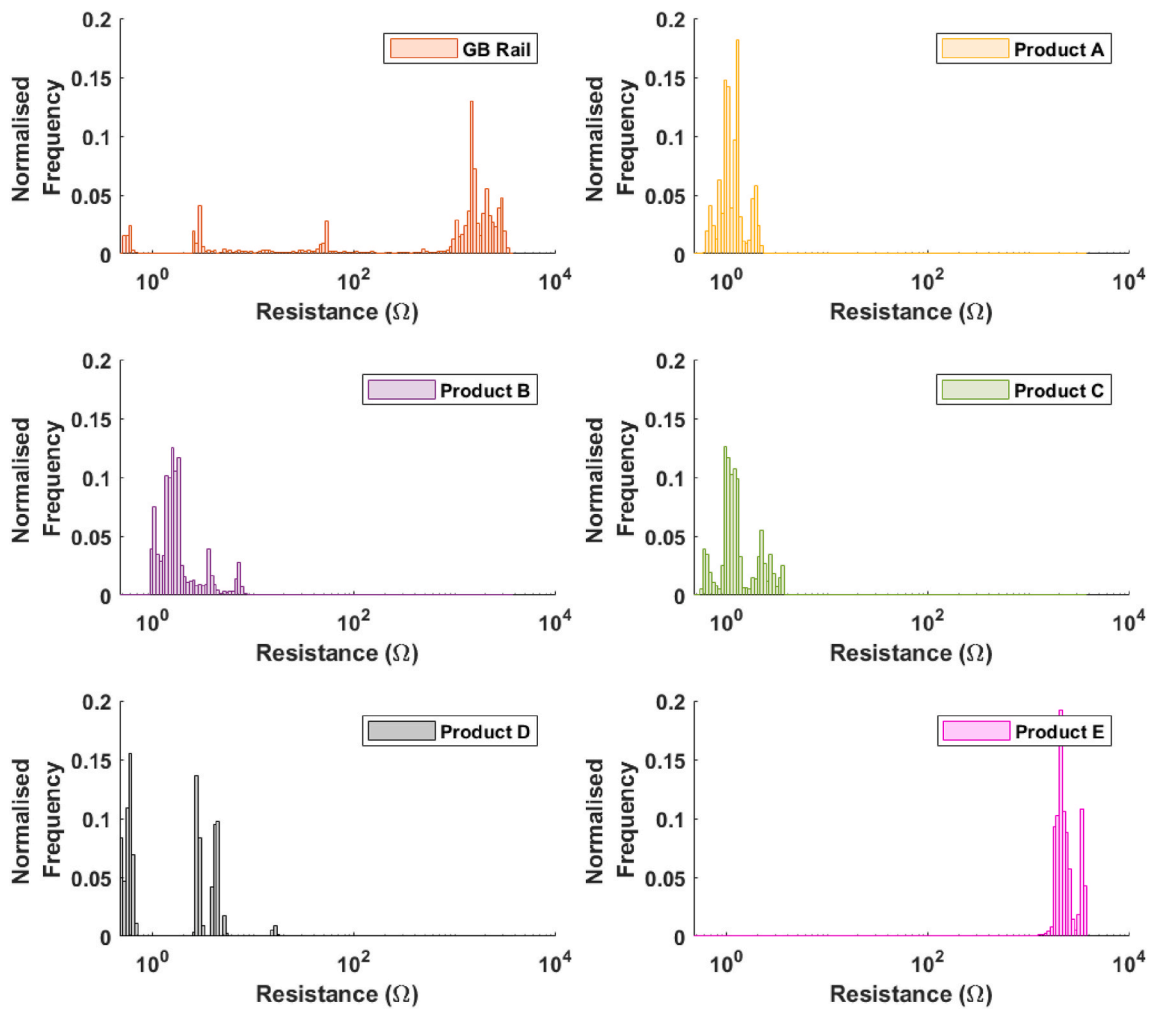


Fig. 23. Histogram plots of time the HPT contact spent at a given resistance in wet conditions with adhesion material over-application.

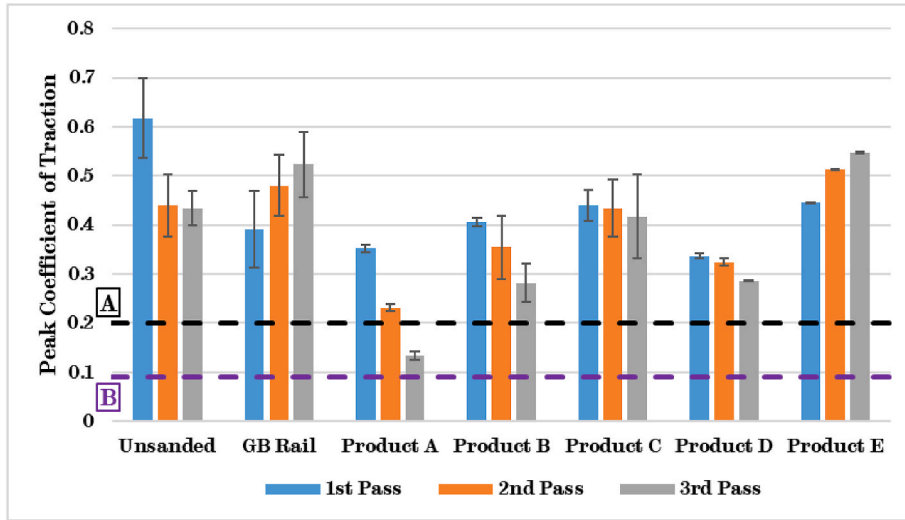


Fig. 24. Peak Coefficient of Traction in Wet Conditions for All Tested Over-Applied Adhesion Materials; (Line A) Minimum Level of Adhesion required for Acceleration, (Line B) Minimum Level of Adhesion required for Braking [1].

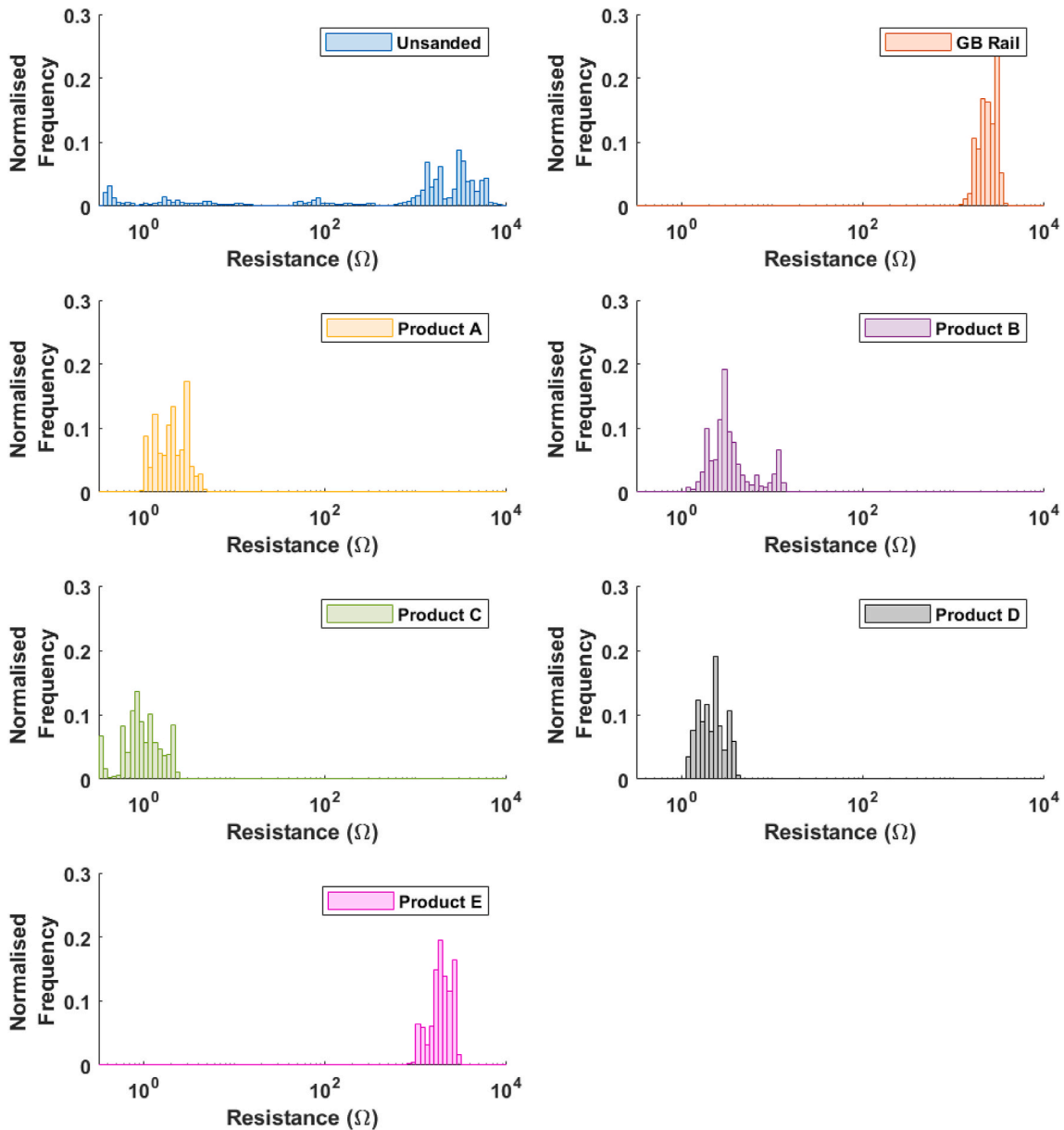


Fig. 25. Histogram plots of time the HPT contact spent at a given resistance in leaf contaminated conditions with adhesion material over-application.

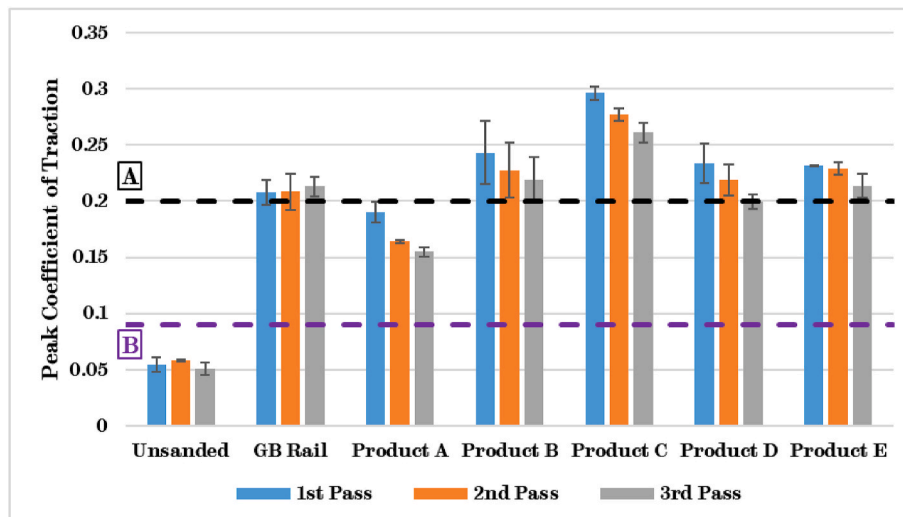


Fig. 26. Peak Coefficient of Traction in Leaf Contaminated Conditions for All Tested Over-Applied Adhesion Materials; (Line A) Minimum Level of Adhesion required for Acceleration, (Line B) Minimum Level of Adhesion required for Braking [1].

will include track testing with a real track circuit, train, and rail, thereby allowing for validation of laboratory findings. Before any future use, an analysis of any potential economic benefit will also be required, though is outside the scope of this work.

Author statement

William Skipper: Methodology, Validation, Formal analysis, Investigation, Writing - Original Draft, Writing - Review & Editing, Visualisation. Sadegh Nadimi: Methodology, Validation, Formal analysis, Investigation, Writing - Review & Editing, Visualisation. Dmitry Gutsulyak: Conceptualisation, Resources, Writing - Review & Editing. Jackie Butterfield: Conceptualisation, Resources, Writing - Review & Editing, Supervision. Tanya Ball: Conceptualisation, Resources, Writing - Review & Editing, Supervision. Roger Lewis: Conceptualisation, Writing - Review & Editing, Supervision, Project administration.

Declaration of competing interest

The authors certify that they have NO affiliations with or involvement in any organization or entity with any financial interest (such as honoraria; educational grants; participation in speakers' bureaus; membership, employment, consultancies, stock ownership, or other equity interest; and expert testimony or patent-licensing arrangements), or non-financial interest (such as personal or professional relationships, affiliations, knowledge or beliefs) in the subject matter or materials discussed in this manuscript.

Data availability

The authors do not have permission to share data.

Acknowledgements

The Authors of this paper would like to thank The Rail Safety Standards Board Cross-Industry R&D Programme for their financial support and guidance of the work (COF-UOS-03). In addition, gratitude should also go to The Royal Academy of Engineering for providing matching funding. For the purpose of open access, the author has applied a Creative Commons Attribution (CC BY) license to any Author Accepted Manuscript version arising.

References

- [1] C.R. Fulford, Review of low adhesion research (T354) (RSSB Report) [Online]. Available: <https://www.sparkrail.org/Lists/Records/DispForm.aspx?ID=9539>, 2004.
- [2] Rail Safety and Standards Board, GMRT2461 sanding equipment (issue 3) [Online]. Available: <https://www.rssb.co.uk/standards-catalogue/CatalogueItem/gmrt2461-iss-3-1>, 2018.
- [3] Rail Accident Investigation Branch, Rail accident report: near miss between a passenger train and cars at norwich road level crossing, new rackheath, norfolk, 24 november 2019 (report 15/2020) [Online]. Available: <https://www.gov.uk/government/news/report-152020-near-miss-between-a-passenger-train-and-cars-at-norwich-road-level-crossing>, 2020. (Accessed 15 December 2020).
- [4] Network Rail, Group Standard GE/RT8250 Class 66 Sanding Defects (NIR 1481), 2002.
- [5] Rail Safety and Standards Board, Research Brief: Review of the Risks and Opportunities from the Application of Sand during Braking (T1046), 2015 [Online]. Available: <https://www.rssb.co.uk/library/research-development-and-innovation/research-brief-T1046.pdf>. (Accessed 12 May 2017).
- [6] W.A. Skipper, A. Chalisey, R. Lewis, A review of railway sanding system research: wheel/rail isolation, damage, and particle application, *J. Rail Rapid Transit* 234 (6) (2019) 567–583.
- [7] O. Arias-Cuevas, Z. Li, R. Lewis, Investigating the lubricity and electrical insulation caused by sanding in dry wheel-rail contacts, *Tribol. Lett.* 37 (3) (2010) 623–635.
- [8] R. Lewis, R.S. Dwyer-Joyce, J. Lewis, Disc machine study of contact isolation during railway track sanding, *J. Rail Rapid Transit* 217 (1) (2003) 11–24.
- [9] M. Evans, W.A. Skipper, L. Buckley-Johnstone, A. Meierhofer, K. Six, R. Lewis, The development of a high pressure torsion test methodology for simulating wheel/rail contacts, *Tribol. Int.* 156 (Apr. 2021), 106842.
- [10] W.A. Skipper, S. Nadimi, A. Chalisey, R. Lewis, Particle characterisation of rail sands for understanding tribological behaviour, *Wear* 432–433 (202960) (2019).
- [11] The British Standards Institution, BS 1377-2:1990 Methods of Test for Soils for Civil Engineering Purposes — Part 2: Classification Tests, British Standard Institution, 1990.
- [12] V. Angelidakis, S. Nadimi, S. Utili, Elongation, Flatness and Compactness Indices to Characterise Particle Form, *Powder Technol.*, Nov., 2021.
- [13] V. Angelidakis, S. Nadimi, S. Utili, SHape Analyser for Particle Engineering (SHAPE): seamless characterisation and simplification of particle morphology from imaging data, *Comput. Phys. Commun.* 265 (2021), 107983.
- [14] Y. Nakata, S. Moriguchi, Round Robin Test of Angle of Repose (AOR), *Universal Benchmark Of DEM Simulation*, 2019 [Online]. Available: <http://geotech.civil.yamaguchi-u.ac.jp/tc105/>.
- [15] H. Saomoto, et al., Round robin test on angle of repose: DEM simulation results collected from 16 groups around the world, *Soils Found.* 63 (1) (Feb. 2023), 101272.
- [16] The British Standards Institution, BS 1377-7:1990 Methods of Test for Soils for Civil Engineering Purposes. Shear Strength Tests (Total Stress), 1990.
- [17] R.J. Marsal, Large scale testing of rockfill materials, *J. Soil Mech. Found Div.* 93 (2) (1967) 27–44.
- [18] British Standards Institution, BS 1377-2:1990 Methods of Test for Soils for Civil Engineering Purposes. Part 2: Classification Tests, British Standard, 1990.
- [19] ASTM, ASTM C702-18: Standard Practice for Reducing Samples of Aggregate to Testing Size, 2018.
- [20] S.J. Blott, K. Pye, Particle shape: a review and new methods of characterization and classification, *Sedimentology* 55 (1) (2008) 31–63.

- [21] H.M.B. Al-Hashemi, O.S.B. Al-Amoudi, A review on the angle of repose of granular materials, *Powder Technol.* 330 (2018) 397–417.
- [22] C.A. Schneider, W.S. Rasband, K.W. Eliceiri, NIH Image to ImageJ: 25 years of image analysis, *Nat. Methods* 9 (7) (Jul. 2012) 671–675.
- [23] W.A. Skipper, S. Nadimi, M. Watson, A. Chalisey, R. Lewis, Quantifying the effect of particle characteristics on wheel/rail adhesion & damage through high pressure torsion testing, *Tribol. Int.* 179 (2022), 108190.
- [24] L. Zhou, H. Brunskill, M. Pletz, W. Daves, S. Scheriau, R. Lewis, Real-time measurement of dynamic wheel-rail contacts using ultrasonic reflectometry, *J. Tribol.* 141 (6) (Jun. 2019).
- [25] W.A. Skipper, R. Lewis, D. Fletcher, Understanding how railhead and wheelset contamination affect track circuit performance: evaluation of datasets (T1222) [Online]. Available: <https://www.sparkrail.org/Lists/Records/DispForm.aspx?ID=27732>, 2023.
- [26] T. Zingg, Beitrag zur Schotteranalyse, ETH Zürich, 1935.
- [27] O. Arias-Cuevas, Z. Li, R. Lewis, A laboratory investigation on the influence of the particle size and slip during sanding on the adhesion and wear in the wheel-rail contact, *Wear* 271 (1–2) (2010) 14–24.
- [28] O. Arias-Cuevas, Z. Li, R. Lewis, E.A. Gallardo-Hernández, Rolling-sliding laboratory tests of friction modifiers in dry and wet wheel-rail contacts, *Wear* 268 (3–4) (2009) 543–551.
- [29] W.J. Wang, T.F. Liu, H.Y. Wang, Q.Y. Liu, M.H. Zhu, X.S. Jin, Influence of friction modifiers on improving adhesion and surface damage of wheel/rail under low adhesion conditions, *Tribol. Int.* 75 (2014).